Analysis on Cost-optimal Deployment of Variable Renewables and Grid Interconnection in Northeast Asia

Takashi Otsuki[1]

Asia Pacific Energy Research Centre (APERC), The Institute of Energy Economics, Japan (IEEJ), Inui Bldg.-Kachidoki 11F, 1-13-1 Kachidoki, Chuo-ku, Tokyo, 104-0054 Japan

Abstract

International grid interconnections have gained attention in Northeast Asia (NEA) as a means to promote variable renewables (VRE), such as wind power and solar PV. This paper quantitatively investigates the benefits of international power transmission for VRE deployment, employing a detailed temporal resolution power system model for NEA. The model determines the optimal hourly dispatch for a single year, which allows us explicit consideration of the power systems characteristics and intermittency of VRE. The results suggest that international transmission may significantly affect VRE deployment in NEA, by promoting wind power in Mongolia and replacing higher-cost solar PV and battery storage otherwise installed in neighboring countries in a "no international transmission" case. However, strict CO_2 emissions regulations, such as 80% reductions, are necessary for implementation. This implies that international transmission of VRE would be an option for long-term deep decarbonization in NEA; the relevant planning organizations need to consider potential feasibility in the context of long-term CO_2 reductions strategies.

Keywords

Northeast Asia; Variable renewables; Super grid; Linear programming.

1.　Introduction

International power grid interconnection has gained attention in Northeast Asia (China, Japan, Korea, Mongolia and Far East region of Russia) over the past two decades. In particular, after the recent air pollution problems in China and the nuclear accident at Fukushima, long-distance international transmissions are highlighted as a means to accelerate the integration of variable renewables (VRE[2])—for example, to connect abundant solar and wind power in Mongolia to the grid—and decarbonize the electricity system [1, 2, 3].

Various analyses of grid interconnection in Northeast Asia have been conducted since at least the 1990s [4, 5, 1, 6, 7, 8]. However, few studies so far have examined the cost-optimal deployment of VRE, or the priority of grid interconnection for the region. For example, Belyaev, et al. [4] and Chung & Kim [5] do not explicitly address VRE in their analysis. Energy Charter, et al. [1], Otsuki, et al. [6] and Otsuki [8] focus on the economics of Mongolian renewables, yet, do not consider VRE in neighboring countries; these analyses, therefore, could not explore the optimal installation of VRE in Northeast Asia. In addition, these analyses employ power generation mix models with a simplified temporal resolution,[3] which might have resulted in underestimating the cost for integration measures.[4] Bogdanov & Breyer [7] discussed the feasibility of a 100% renewable power system, using an optimization model with an hourly temporal resolution for a year. This analysis implies that international transmission contributes to curbing the cost of achieving a 100% renewable power supply. However, the priority of international transmission as an electricity supply option—for example, the condition, such as the level of environmental policies, where interconnection should be implemented—was not fully analyzed in that study.

Therefore, the author developed an optimal power generation mix model with an hourly temporal resolution to analyze the optimal installation of VRE and the priority of grid interconnection in Northeast Asia. Although there exist uncertainties regarding the degree of future energy cooperation in Northeast Asia due to geopolitical issues, this paper can contribute to stakeholders' and policy makers' discussions by showing economic implications in a quantitative manner.

This paper proceeds as follows: Section 2 gives an overview of the optimal power generation mix model; Section 3 presents the simulation results; and Section 4 summarizes major conclusions and implications, and then proposes a future research agenda.

---

[2] This paper defines VREs as solar PV and onshore wind.
[3] Energy Charter, et al. [1] does not explicitly consider load curves nor supply-demand balance. Otsuki, et al. [6] and Otsuki [8] only model seasonal load curves (one calendar year is decomposed into 120 time segments = 24h per day × 1 representative day per season × 5 seasons per year).
[4] According to IRENA [38], generation expansion models with limited time slices tend to, for example, underestimate the economics of flexible dispatchable generation.

2. Method

2.1. Overview

This paper developed an NEA-wide multi-region optimal power generation mix model, referring to Otsuki [8] and Komiyama, et al. [9] (Fig.1 and Appendix 1 for detailed formulation). This is a linear programming model, which determines cost-optimal power generating capacity and hourly operation through minimizing annual total system cost for Northeast Asia. Total system cost in this model includes capital, operation and maintenance (O&M) and fuel costs for generation, storage and inter-regional transmission technologies. This model uses capital recovery factors, assuming a discount rate of 5%, to annualize capital cost for modeled technologies. This model takes into account nine types of generation (solar PV, wind, hydro, nuclear, coal-fired, gas-fired, oil-fired, hydrogen turbine, and fuel cell), three types of storage (pumped hydro, battery, and compressed hydrogen tank), and one intra-regional transmission technology (HVDC = High Voltage Direct Current). This paper assumes water electrolysis for hydrogen production.

The model divides Northeast Asia into fifteen nodes (Fig.2), represented by eleven city nodes and four supply nodes. City nodes have electricity demand as well as generation and storage facilities, while supply nodes have only generation and/or storage facilities to export to neighboring nodes. Hydro plants are considered in the China Three-Gorges (PRC-TG) node, while solar PV and wind turbine in the other three supply nodes. Branches in Fig.2 indicate assumed transmission routes. This study formulates inter-regional transmission as a transport problem, keeping the optimization problem linear and optimizing grid extensions, generation expansion as well as their operations simultaneously. Transmission distance is estimated based on airline distance plus 20% for possible route circuity.
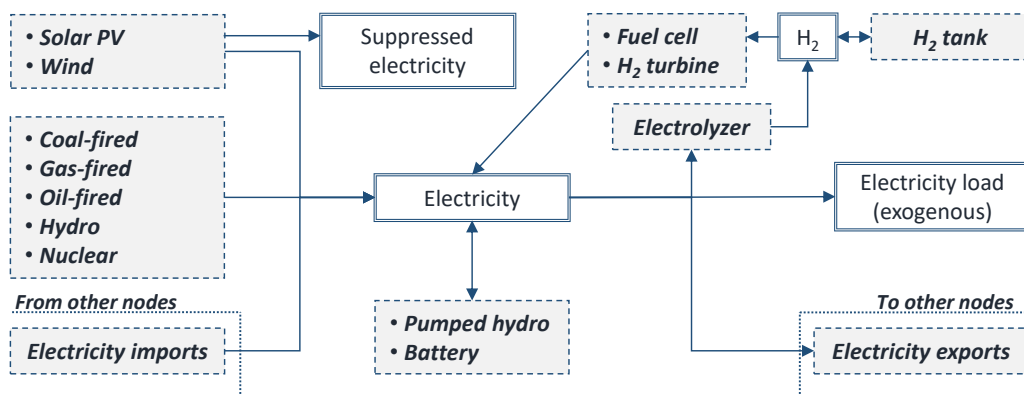

Fig.1 Schematic diagram of the optimal power generation mix model for Northeast Asia. Note: H_2 indicates hydrogen.
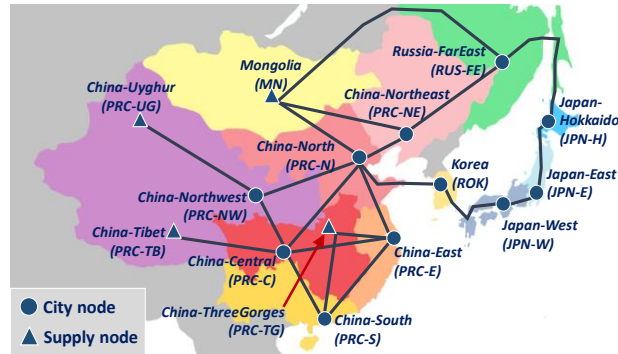
Fig.2 Regional division and assumed transmission route

From the viewpoint of grid stability, this model limits the level of system non-synchronous penetration (SNSP) as formulated in Eq. A30. Non-synchronous power in this paper includes VRE, fuel cell, battery and inter-regionally transmitted power. The assumption of the maximum SNSP in Section 3 is 75%, based on a study in Ireland[5] [10, 11]. However, it is important to note that the maximum limit may depend on each grid's individual characteristics. Further studies, together with actual operating experiences, would be necessary to determine the appropriate level in Northeast Asian countries. Future work is necessary to perform a sensitivity analysis to investigate the effects of the SNSP limit on the generation mix and VRE deployment in Northeast Asia.

2.2. Case setting

This paper examines seven cases as summarized in Table **1**. The simulated year in this study is 2030. The *Base* case does not allow international grid enhancement or limit CO_2 emissions. The *Domestic* cases (three cases) do not assume international grid extension, but three levels of CO_2 emissions regulation for the whole region: -25%, -50% and -80% from the *Base* case. The *International* cases (three cases) consider international grid extension as well as three levels of emissions regulation.

General assumptions for the modelled technologies are as follows: nuclear, hydro and pumped hydro capacity are imposed exogenously, and the model determines the capacity of other technologies as well as hourly operation of all technologies based on cost-minimization. Therefore, as nuclear and hydro capacity are exogenous variables in this study, the model attempts to satisfy the CO_2 regulation by shifting to cleaner fossil fuels and expanding VRE.

2.3. Input data assumptions
2.3.1. Electricity load curves

Hourly load curves for a year in Japan, Korea and Russia were obtained from the governments, electricity system operators or market operators [12, 13, 14]. These load curves were adjusted by referring

---

[5] EirGrid, stated-owned transmission system operator in Ireland, has limited the SNSP below 50% since 2011 [10], and increased the limit to 60% as a trial since November 2016 with an ultimate aim of 75% by 2020 [11].

to the projected electricity consumption for 2030 [15]. Actual load curves in China are not publicly available; this study therefore estimated them using available data (Appendix 2).

2.3.2.   Generation and storage technologies

Nuclear, hydro and pumped hydro capacity are given, referring to the projected capacity for 2030[6] [15], while capacity of other technologies, such as VRE and fossil fuel plants, are determined by the model. Initial values are based on the 2030 capacity for VRE [15] and on the actual capacity in 2010 for other technologies[7].

Economic and technical assumptions were obtained from Komiyama, et al. [16] for the hydrogen systems (electrolyzer, compressed hydrogen tank and hydrogen turbine), METI [17] for pumped hydro and battery, and IEA [18] and Komiyama & Fujii [19] for other technologies (see A1.3 for detailed assumptions). Table 2 shows capital cost assumptions for VRE technologies, as an example; this study assumed 400 USD/kWh for battery cost. VREs' hourly output profiles in each node were estimated based on the methods presented in Komiyama, et al. [9]. This study used the meteorological data in NREL [20], JMA [21] and KMA [22] for China, Japan and Korea, respectively. Solar radiation data for Mongolia is from NREL [23]; but, as for wind speed, due to data availability, this paper used the data from the Inner Mongolia region in China [20] as a proxy. Meteorological data for the Russia Far East region is also limited; thus, this study referred to data from Chinese observation points near the China-Russia border [20]. Estimated capacity factors are described in Table 2; the factor varies by node and this table shows the range in each country. Assumed installation potential for VRE are based on [24, 25] for China, MOE [26] for Japan, KOPIA [27] and Kim, et al. [28] for Korea, and Charter, et al. [1] and Elliott, et al. [29] for Mongolia. Assumed upper limits for solar PV are 39,400 GW in China, 339 GW in Japan, 25 GW in Korea and 1,500 GW in Mongolia, and for wind power 1,800 GW, 286 GW, 41 GW and 1,100 GW, respectively.

2.3.3.   Inter-regional transmission technology

This study estimated the cost for transmission, assuming HVDC overhead line for overland transmission and HVDC cable for undersea transmission. AC-DC conversion stations were installed at the each end of the interconnection. A cost of 4.2 million USD/km (M USD/km) was assumed for HVDC overhead lines (rated power: 3 GW), 7.2 M USD/km for HVDC undersea cable (rated power: 3 GW) and 300 M USD/GW/station for AC-DC conversion stations. Assumed lifetime, transmission losses, AC-DC conversion losses and annual fixed O&M cost were 40 years, 5%/1000 km, 1.5%/station and 0.3% in a ratio to initial cost for all line types, respectively. Initial values for transmission capacity are based on the 2010 actual capacity; for example, Chen, et al. [30] for domestic transmission capacity in China.

---

[6] This paper refers to the BAU Scenario in APERC [15], which includes current policies and trends.
[7] In summary, this paper uses the 2010 actual capacity as Initial values for all generation, storage and transmission technologies except for VRE, nuclear, hydro and pumped hydro.

Table 1 Case setting

	Base case	*Domestic* cases (3 cases)	*International* cases (3 cases)
Domestic grid	Extension allowed for all cases		
International grid	Extension not allowed		Allowed
CO_2 emissions regulation	No limit	-25%, -50% and -80% from the *Base* case	

Table 2 Assumptions for capital cost (top, in USD/kW) and capacity factor (bottom, in %) of solar PV and wind power

	China	Japan	Korea	Mongolia	Russia FarEast
Solar PV	1380	2400	2400	1430	1400
	12-18%	11-16%	12%	15%	13%
Wind turbines	1150	2000	2000	1150	1930
	10-29%	20-22%	19%	24%	20%

3. Results and discussion

3.1. Generation mix

International interconnection would significantly affect cost-optimal VRE deployment in Northeast Asia under strict CO_2 emissions regulation, such as 50% and 80% reductions (Fig.3a). In the *Domestic* cases, wind power shows a saturating trend after 25% CO_2 reduction, as it reaches a techno-economic installation limit. Thus, the region achieves further emissions reduction by expanding solar PV. On the other hand, in the *International* cases, wind power grows even under the 50% and 80% CO_2 reduction. For example, under 80% reduction, the share of wind doubles from 16% in the *Domestic* to 33% in the *International* case. Mongolia (MN) expands wind power for electricity exports, largely affecting the generation mix in neighboring countries, in particular, China because of its large market size (Fig.3b). In the *International (50% reduction)* case, China imports wind power from Mongolia to reduce emissions, rather than shifting fossil fuels from coal to gas (this is why gas and coal show a negative and positive value, respectively, under the 50% CO_2 reduction in Fig.3b). Under 80% reduction, wind power in Mongolia (total 1,100 GW) replaces solar PV in China, especially PRC-N (China-North).

In contrast, the results also imply modest impacts of international interconnection under 25% reduction (Fig.3b). This is because the region can meet the emissions reduction mostly by domestic VRE. As mentioned in the previous paragraph, international interconnection has significant effects on VRE deployment and the generation mix in Northeast Asia, through providing access to wind power in Mongolia; yet, strict emissions reduction policy would be necessary for implementation.

(a) Generation mix
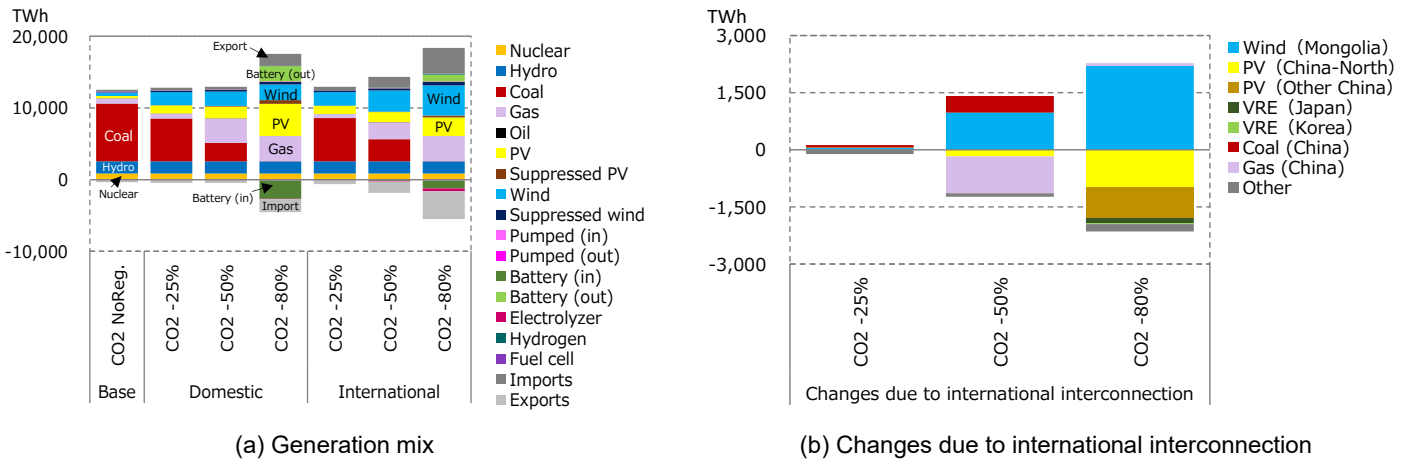
(b) Changes due to international interconnection

Fig.3 Generation mix in Northeast Asia

Fig.4 illustrates the hourly supply-demand profile in January in PRC-N (China-North), where international interconnection would affect the generation mix significantly (as shown in Fig.3b). Coal-fired generation accounts for the major share in the *Base* case; ramping operation of fossil-fuel plants contributes to integrating VRE. Fig.4b shows the massive growth of solar PV in the *Domestic (80% reduction)* case. In order to manage excess generation during daytime, various measures, including the ramping operation of power plants, charging into battery, transmission to PRC-E (China-East), as well as suppression control, are dynamically combined. Whereas, the *International (80% reduction)* case shows large-scale imports from MN and exports to PRC-E (Fig.4c). Electricity imports replace solar PV, reducing daytime excess generation and lowering the need for storage. Note that the node operates gas-fired generation even in the 80% reduction cases to satisfy the SNSP constraint (see Section 2.1 and Eq. A30).

Battery becomes the prevailing storage technology in the *Domestic* cases, especially under 80% reduction regulation, to store excess generation from solar PV (Fig.5). In China, battery power-capacity and energy-capacity reach 1,540 GW and 9,230 GWh, respectively. Cycle efficiency of battery technologies is, in general, superior to other storage technologies, such as hydrogen storage, and thus suitable for frequent daily cyclic operation for solar PV. In the *International (80% reduction)* case, Mongolia installs battery as well as hydrogen storage to manage wind's intermittency. Fig.6a-b illustrate that battery is operated for diurnal storage, while hydrogen storage is for longer-term, like weekly, storage since a compressed hydrogen tank has lower storage losses (as also pointed out in Komiyama, et al. [9]). This implies that the choice of optimal storage technology depends on technical characteristics as well as operation patterns.
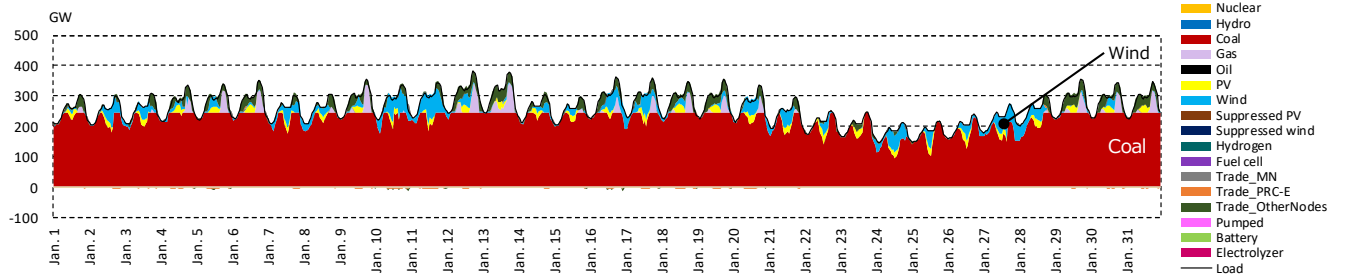
(a) *Base* case
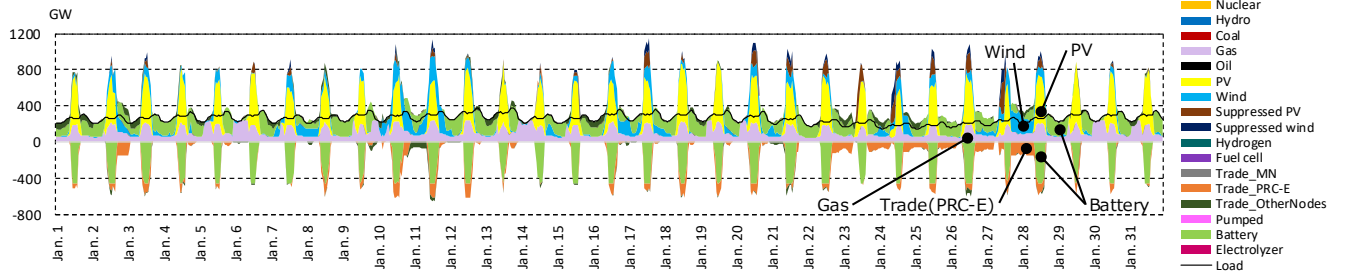
(b) *Domestic* case (80% CO_2 reduction from the *Base*)
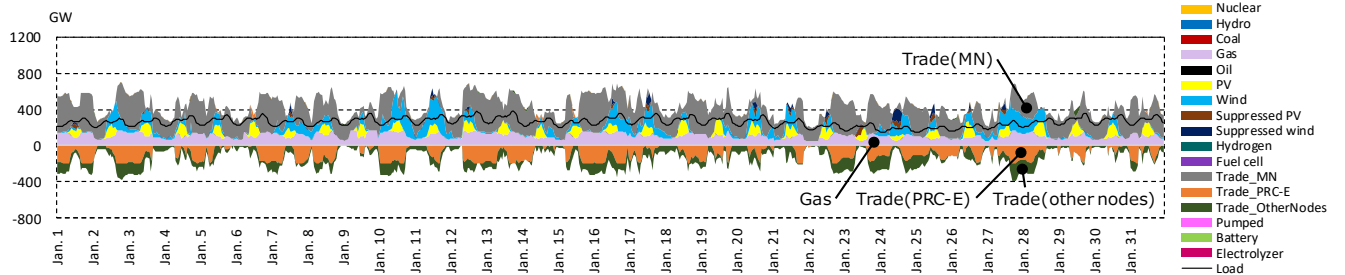
(c) *International* case (80% CO_2 reduction from the *Base*)

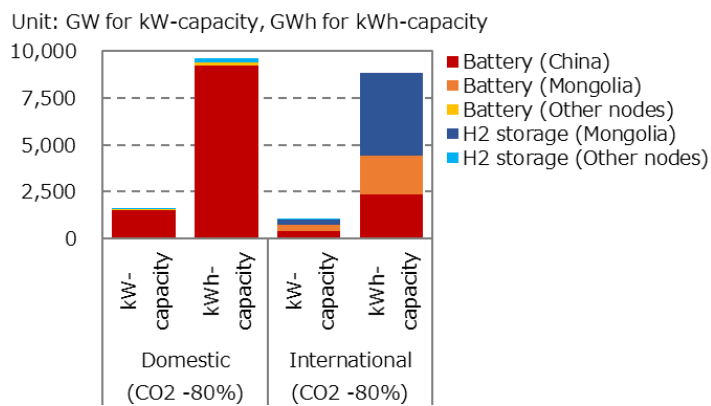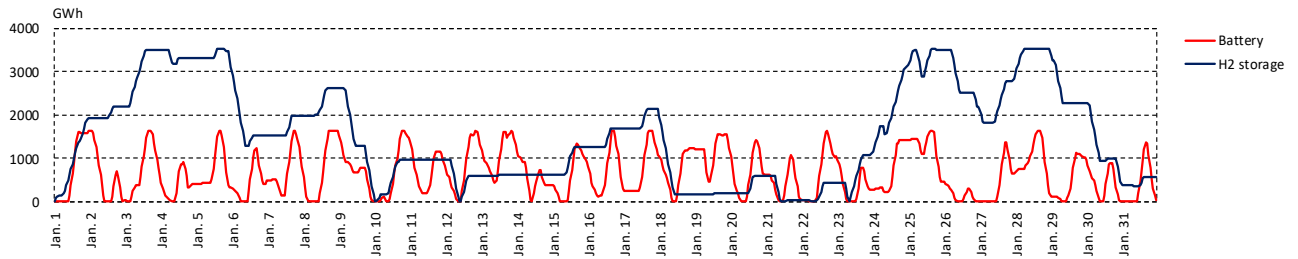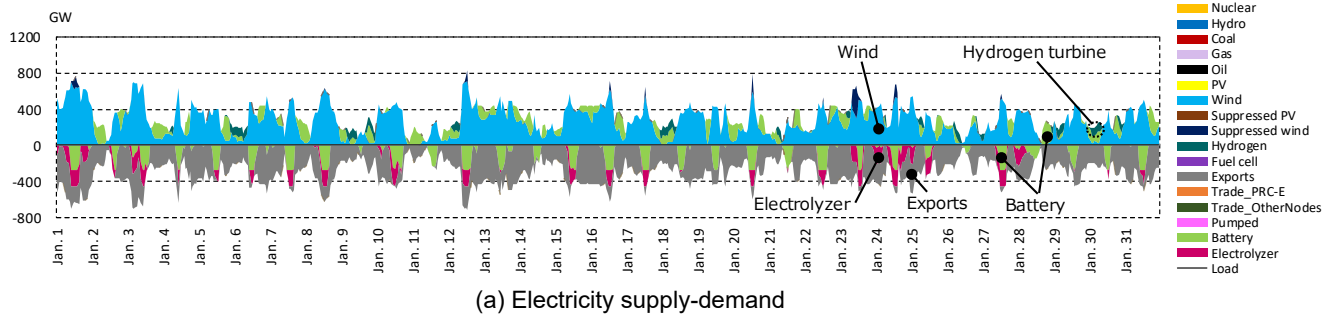Fig.4 Hourly electricity supply-demand profile in January, China-North (PRC-N)

Fig.5 Battery and H_2 storage capacity

(*Domestic* and *International* cases under 80% CO_2 reduction from the *Base*)

(a) Electricity supply-demand

(b) Stored electricity in battery and H_2 storage system
Fig.6 Hourly operational profile in the *International* case under 80% reduction, January, Mongolia

3.2. Inter-regional transmission

Inter-regional transmission is relatively modest in the *Base* case, except for the following routes in China: from PRC-NE (China-Northeast) to PRC-N (China-North) and from PRC-TG (China-Three Gorges) to PRC-E (China-East) to transmit wind and hydro power, respectively (Fig.7a).

Transmission capacity grows to access VRE resources under stricter CO_2 regulation (Fig.7b-c). In the *Domestic (80% reduction)* case, China enhances its transmission network from wind-rich nodes, such as PRC-N and PRC-NW (China-Northwest), to large demand centers, including PRC-E and PRC-C. The result also implies the need for nationwide transmission infrastructure for Japan to utilize abundant wind resources in JPN-H (Japan-Hokkaido). Wind power capacity in JPN-H reaches 109 GW, equivalent to 70% of wind power potential in Hokkaido [26]. The assumed peak load in JPN-H is 7 GW; that level of wind installation would bring significant changes in the node.

In the *International (80% reduction)* case, inter-regional transmission notably expands from MN to PRC-N, from PRC-N to PRC-E and from PRC-N to ROK (Fig.7c); net transmitted electricity on these routes reaches a significant[8] level: 860 TWh, 840 TWh/yr and 220 TWh/yr, respectively. Transmission also increases between Japan and Korea (68 TWh/yr from ROK to JPN-W, and 10 TWh/yr in the other direction), although its scale is modest compared with Mongolia-China and China-Korea, implying larger opportunities for China, Korea and Mongolia.

---

[8] Assumed electricity demand in PRC-N, PRC-E and ROK is 2,470TWh/yr, 2,590TWh/yr and 660TWh/yr, respectively.
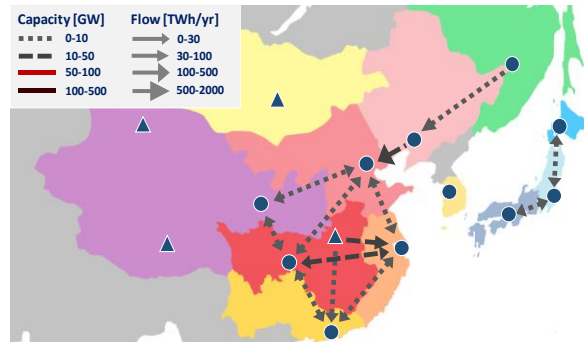
(a) *Base* case
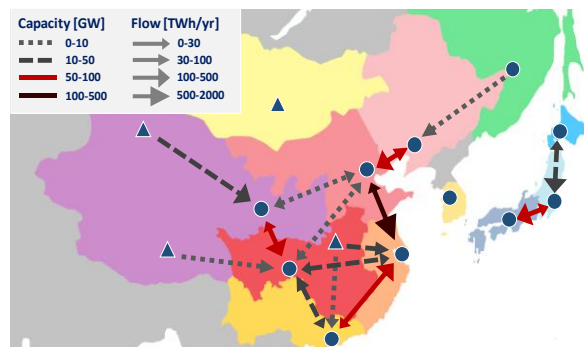
(b) *Domestic* case (80% CO_2 reduction from the *Base*)
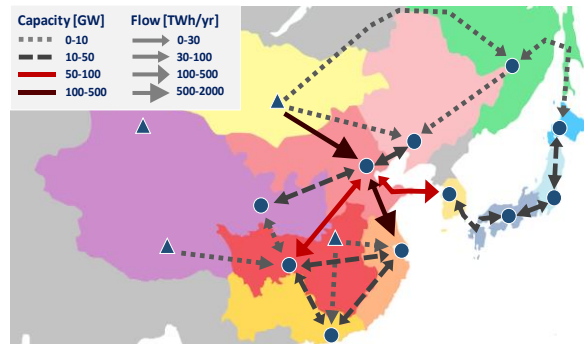
(c) *International* case (80% CO_2 reduction from the *Base*)

Fig.7 Inter-regional transmission capacity and flow

3.3. Total system cost and marginal abatement cost

International transmission of VRE contributes to curbing the cost for emissions reduction, in particular, under regulation stricter than 50% reduction (Fig.8). The economic benefits due to reduced total cost are relatively modest—savings of 0.3% and 1.6%—from the *Domestic* to the *International* cases under 25% and 50% emissions constraints, respectively, and expand to 11% under 80% CO_2 reduction. The cost saving under 80% reduction is mainly due to curbing capital cost for VRE and battery; even though the region needs to invest in inter-regional transmission facilities, benefits from access to cost-competitive

VRE in neighboring countries as well as less need for battery capacity are estimated to exceed the cost for transmission. These results also suggest that cost-competitiveness of international transmission would be enhanced by the lower cost of VRE in neighboring countries and transmission facilities, whereas undermined by improved economics of domestic VRE, especially solar PV, and battery storage.

The economic benefit implied by the model under 50% reduction, a saving of 1.6%, was relatively modest, although wind power is largely installed in Mongolia (Fig.3b). This trend is also illustrated in Fig.9; CO_2 marginal abatement cost is also notably curbed under the 80% reduction regulation, yet not under 50%. Strong emission policies, such as 80% reduction, would be necessary for international transmission of VRE to be attractive from an economic viewpoint.
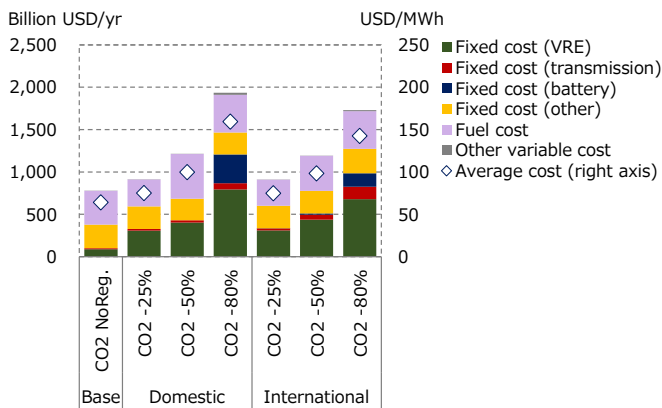

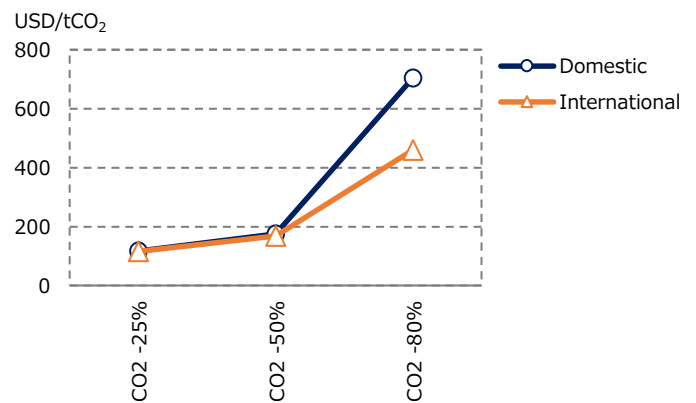Fig.8 Annual total system cost and average generation cost

Fig.9 CO_2 marginal abatement cost

4.   Conclusion and future work

This paper discusses the impacts of international interconnection on cost-optimal deployment of VRE in Northeast Asia, employing a multi-region optimal power generation mix with an hourly temporal resolution. The results suggest that international interconnection would significantly affect VRE deployment in Northeast Asia, by promoting wind power in Mongolia and replacing higher-cost solar PV and battery storage otherwise installed in the *Domestic* cases. However, strict CO_2 emissions regulations, such as 80% reductions from the *Base*, are necessary for implementation. This implies that international transmissions of VRE would be an option for long-term deep decarbonization in NEA; the relevant planning organizations need to consider potential feasibility in the context of long-term CO_2 reductions strategies.

Future work should include modeling and analysis on energy security perspectives. This paper assumes that the Northeast Asia countries fully cooperate for regional optimization in order to quantify the cost-optimal deployment of VRE. Therefore, emergency situations, such as the disruption of electricity trade due to technical or political issues, were outside of the scope of this research. Incorporating energy security aspects into the model, for example, by using stochastic programming techniques, would be an

important research contribution to comprehensively understand the opportunities and barriers for grid interconnection.

Acknowledgement

Appendix 1. Model formulation and assumptions

This section describes the equations of the model in detail in order to provide a detailed understanding of this study. The model is formulated as a linear programming problem that aims to minimize annual total system cost for Northeast Asia. Table A1 shows the endogenous variables of the model.

Table A1 Endogenous variables of the multi-region power generation mix model

z	Total annual cost [USD/yr]
cf_n	Annual fixed cost at node n [USD/yr]
cv_n	Annual variable cost at node n [USD/yr]
$kg_{n,i}$	Capacity of generation type i at node n [kW]
$akg_{n,i,d}$	Available capacity of generation type i in day d at node n [kW]
$mkg_{n,i,m}$	Capacity of generation type i maintained under schedule m [kW]
$ks1_{n,s}$	kW-capacity of storage type s at node n [kW]
$ks2_{n,s}$	kWh-capacity of storage type s at node n [kWh]
$kl_{n,n2,l}$	Capacity of transmission type l between nodes n and $n2$ [kW]
ke_n	Capacity of electrolyzer at node n [kW]
$xg_{n,i,d,t}$	Output of generation type i at local time t in day d at node n [kW]
$mxg_{n,i,d}$	Maximum output level of generation type i in days d and $d+1$ at node n [kW]
$dg_{n,i,d,t}$	Suppressed output of generation type i (i=solar PV or wind) at local time t in day d at node n [kW]
$sch_{n,s,d,t}$	Electricity charge of storage type s at local time t in day d at node n [kW]
$sdc_{n,s,d,t}$	Electricity discharge of storage type s at local time t in day d at node n [kW]
$xss_{n,s,d,t}$	Stored electricity type s at local time t in day d at node n [kWh]
$xl_{n,n2,l,d,t}$	Transmitted power from nodes n to $n2$ via transmission type l at time t in day d (node n time) [kW]
$xe_{n,d,t}$	Output of electrolyzer (hydrogen production) at local time t in day d at node n [kW]

where:

$n, n2$: *node index* $(1: PRC - NE, 2: PRC - N, 3: PRC - E, 4: PRC - C, 5: PRC - NW, 6: PRC - S, 7: PRC - TG,$
$8: PRC - UG, 9: PRC - TB, 10: JPN - H, 11: JPN - E, 12: JPN - W, 13: ROK, 14: RUS - FE, 15: MN)$

d: *day index* $(0, 1, …, 364 \text{ or } 365)$, t: *time index* $(0, 1, …, 23)$, m: *maintenance schedule index* $(0,1,2,3)$

i: *generation technology index* $(1: Solar\ PV, 2: Wind, 3: Hydro, 4: Nuclear, 5: Coal - fired, 6: Gas - fired,$
$7: Oil - fired, 8: Hydrogen\ turbine, 9: Fuel\ cell)$

s: *storage technology index* $(1: Pumped\ hydro, 2: Battery, 3: Compressed\ hydrogen\ tank)$

l: *transmission technology index* $(1: HVDC\ transmission)$

A1.1. Objective function

The objective function—annual total system cost for Northeast Asia—is formulated as Eq. A1-Eq. A3. Total system cost consists of fixed cost and variable cost. Fixed cost includes capital cost as well as O&M cost for generation, storage, transmission and electrolyzer. Variable cost is modelled as the following two components: fuel cost for generation and cost for consumable material in battery technologies.

$$min. \ z = \sum_n (cf_n + cv_n)$$

Eq. A1

$$cf_n = \sum_i AG_i \cdot CG_{n,i} \cdot kg_{n,i} + \sum_s AS_s \cdot \left(CS1_{n,s} \cdot ks1_{n,s} + CS2_{n,s} \cdot ks2_{n,s}\right)$$

Eq. A2

$$+ \sum_{n2>n} \sum_l AL_l \cdot CL_{n,n2,l} \cdot kl_{n,n2,l} + AE \cdot CE \cdot ke_n$$

$$cv_n = \sum_i \left(FG_{n,i} \cdot \sum_d \sum_t \frac{xg_{n,i,d,t} \cdot HW}{EffG_{n,i}}\right) + \sum_s \left(VS_{n,s} \cdot \sum_d \sum_t sch_{n,s,d,t} \cdot HW\right)$$

Eq. A3

where: AG_i: annual fixed charge rate (calculated from capital recovery factor and annual O&M cost rate) for generation type i at node n; $CG_{n,i}$: capital cost for generation type i at node n [USD/kW]; AS_s: annual fixed charge rate for storage type s; $CS1_{n,s}$: capital cost for kW-capacity of storage type s at node n [USD/kW]; $CS2_{n,s}$: capital cost for kWh-capacity of storage type s at node n [USD/kWh]; AL_l: annual fixed charge rate for transmission type l; $CL_{n,n2,l}$: capital cost for transmission type l between node n and node $n2$ [USD/kW]; AE: annual fixed charge rate for electrolyzer; CE: capital cost for electrolyzer [USD/kW]; $FG_{n,i}$: fuel cost for generation type i at node n [USD/kWh]; $FffG_{n,i}$: conversion efficiency of generation type i at node n [USD/kWh]; $VS_{n,s}$: Consumable material (electrode, electrolyte and separator) cost for battery [USD/kWh]; HW: time slot length (HW=1 hour in this study).

A1.2. Constraints

A1.2.1. Power demand and supply balance

Eq. A4 ensures that electricity demand must be satisfied at all times in all days and at all nodes. The left part indicates the sum of power supply from generators, electricity consumption for water electrolysis, net power imports and net power discharge of storage technologies. Time differences between power exporting and importing nodes are considered as DA and TA in Eq. A4.

$$\sum_i xg_{n,i,d,t} - \frac{xe_{n,d,t}}{EffE_n} + \sum_{n2} \sum_l \left(xl_{n2,n,l,DA_{n2,n,d,t},TA_{n2,n,t}} \cdot EffL_{n2,n,l} - xl_{n,n2,l,d,t}\right)$$

Eq. A4

$$+ \sum_{s=1}^{2} \left(xdc_{n,s,d,t} - xch_{n,s,d,t}\right) = L_{n,d,t}$$

$$EffL_{n,n2,l} = (1 - LL_l)^{DIS_{n,n2}}$$

Eq. A5

where: $L_{n,d,t}$: electric load at time t in day d at node n [kW]; $EffE_n$: conversion efficiency of electrolyzer at node n; $EffL_{n,n2,l}$: transmission efficiency for transmission type l between nodes n and $n2$; LL_l: transmission loss for transmission type l between node n and $n2$ [per thousand km]; $DIS_{n,n2}$: transmission distance between nodes n and $n2$ [thousand km]; $DA_{n2,n,d,t}$ and $TA_{n2,n,t}$: local time (day and time, respectively) at the origin of electricity imports.

A1.2.2.   Hydrogen energy balance

Eq. A6 is to balance hydrogen production and consumption. The left part indicates the sum of hydrogen production in electrolyzer and net discharge of hydrogen tank, while the right part describes consumption for hydrogen turbine or fuel cell.

$$xe_{n,d,t} + \left(xdc_{n,3,d,t} - xch_{n,3,d,t}\right) = \sum_{i=8}^{9} \frac{xg_{n,i,d,t}}{EffG_{n,i}} \qquad \text{Eq. A6}$$

A1.2.3.   Stored energy balance

Eq. A7 relates power charge (xch), power discharge (xdc) and the level of stored electricity (xss). Self-discharge loss and charge/discharge efficiency are considered in this equation.

$$xss_{n,s,d,t+1} = xss_{n,s,d,t} \cdot (1 - LS_s) + \left(\sqrt{EffS_s} \cdot xch_{n,s,d,t} - \frac{xdc_{n,s,d,t}}{\sqrt{EffS_s}}\right) \cdot HW \qquad \text{Eq. A7}$$

where: LS_s: self-discharge rate for storage type s; $EffS_s$: cycle efficiency of storage type s.

A1.2.4.   Installable capacity constraint

Installable capacity of each technology is constrained by its minimum and maximum deployable limits.

$$MinKG_{n,i} \leq kg_{n,i} \leq MaxKG_{n,i} \qquad \text{Eq. A8}$$

$$MinKS1_{n,s} \leq ks1_{n,s} \leq MaxKS1_{n,s} \qquad \text{Eq. A9}$$

$$ks2_{n,s} = RS_s \cdot ks1_{n,s} \quad (s = 1, 2) \qquad \text{Eq. A10}$$

$$MinKL_{n,n2,l} \leq kl_{n,n2,l} \leq MaxKL_{n,n2,l} \qquad \text{Eq. A11}$$

$$MinKE_n \leq ke_n \leq MaxKE_n \qquad \text{Eq. A12}$$

where: $MinKG_{n,i}$: initial capacity for generation type i at node n [kW]; $MaxKG_{n,i}$: capacity upper limit for generation type i at node n [kW]; $MinKS1_{n,s}$: initial kW-capacity for storage type s at node n [kW]; $MaxKS1_{n,s}$: kW-capacity upper limit for storage type s at node n [kW]; RS_s: kWh-capacity ratio to kW-capacity (pumped hydro and battery); $MinKL_{n,n2,l}$: initial transmission capacity for transmission type l between nodes n and $n2$ [kW]; $MaxKL_{n,n2,l}$: capacity upper limit for transmission type l between nodes n and $n2$ [kW]; $MinKE_n$: initial capacity for electrolyzer at node n [kW]; $MaxKE_n$: capacity upper limit for electrolyzer at node n [kW].

A1.2.5. Output constraint

Eq. A13-Eq. A19 constrain output of generation, storage, transmission and electrolyzer. For solar PV and wind, the hourly output availability profiles (*UG1*) are exogenously given in Eq. A13. The left part of Eq. A13 indicates two destination for output power from wind and solar PV: power supplied to the grid (*xg*) or suppressed (*dg*). Eq. A14 models the output of hydro power and fuel cell. The other types of power generation technologies are constrained to their available capacity (Eq. A15). Eq. A16 constrains the charge to or discharge from storage facilities to their available power capacity (kW-capacity). Eq. A17 constrains stored electricity to the energy capacity (kWh-capacity) of the facility, i.e., reservoir capacity for pumped hydro. Eq. A18 and Eq. A19 are for the output of transmission facilities and electrolyzer, respectively.

$$xg_{n,i,d,t} + dg_{n,i,d,t} = UG1_{n,i,d,t} \cdot kg_{n,i} \quad (i = 1, 2) \qquad \text{Eq. A13}$$

$$xg_{n,i,d,t} \leq UG2_{n,i} \cdot kg_{n,i} \quad (i = 3, 9) \qquad \text{Eq. A14}$$

$$xg_{n,i,d,t} \leq akg_{n,i,d} \quad (i = 4, 5, \dots, 8) \qquad \text{Eq. A15}$$

$$xch_{n,s,d,t} + xdc_{n,s,d,t} \leq US_s \cdot ks1_{n,s} \qquad \text{Eq. A16}$$

$$xss_{n,s,d,t} \leq US_s \cdot ks2_{n,s} \qquad \text{Eq. A17}$$

$$xl_{n,n2,l,d,t} + xl_{n2,n,l,d,t} \leq UL_l \cdot kl_{n,n2,l} \qquad \text{Eq. A18}$$

$$xe_{n,d,t} \leq UE \cdot ke_n \qquad \text{Eq. A19}$$

where: $UG1_{n,i,d,t}$: output profile of variable renewable (solar PV and wind) energy at local time *t* in day *d* at node *n*; $UG2_{n,i}$: availability factor of hydro power and fuel cell at node *n*; US_s: availability factor of storage type *s*; UL_l: availability factor of transmission type *l*; UE: availability factor of electrolyzer.

A1.2.6. Ramping constraint for thermal generation

The model considers technology-specific ramping constraints for thermal plants (nuclear, coal-fired, gas-fired, oil-fired, and hydrogen turbine). For technical reasons, each technology has its own controllability, with output of these generators changeable within their ramping capabilities. Ramping up and ramping down limits are modeled as follows in this study:

$$xg_{n,i,d,t+1} \leq xg_{n,i,d,t} + RampUp_i \cdot akg_{n,i,d} \quad (i = 4, 5, \dots, 8) \qquad \text{Eq. A20}$$

$$xg_{n,i,d,t+1} \geq xg_{n,i,d,t} - RampDn_i \cdot akg_{n,i,d} \quad (i = 4, 5, \dots, 8) \qquad \text{Eq. A21}$$

where: $RampUp_i$: maximum ramp up rate per unit of time for generation type *i*; $RampDn_i$: maximum ramp down rate per unit of time for generation type *i*.

A1.2.7. Minimum output constraint for thermal generation

Eq. A22 requires that thermal plants, excluding the plants served as DSS (Daily Start and Stop) generators (*DssG*), generate electricity at no less than their minimum output threshold. The right-hand side value of Eq. A22, which is a multiplication of available plant's capacity without DSS mode (*mxg-DssG*akg*) and a ratio of minimum output level (*MolG*), corresponds to the minimum output level of each generation

type. Maximum output level (*mxg*) is estimated through Eq. A23 and Eq. A24.

$$xg_{n,i,d,t} \geq \left(mxg_{n,i,d} - DssG_i \cdot akg_{n,i,d}\right) \cdot MolG_i \quad (i = 4, 5, \ldots, 8) \qquad \text{Eq. A22}$$

$$mxg_{n,i,d} \geq xg_{n,i,d,t} \quad (i = 4, 5, \ldots, 8) \qquad \text{Eq. A23}$$

$$mxg_{n,i,d} \geq xg_{n,i,d+1,t} \quad (i = 4, 5, \ldots, 8) \qquad \text{Eq. A24}$$

where: *DssG_i*: share of daily start and stop operation (DSS) of generation type *i*; *MolG_i*: minimum output rate of operation for generation type *i*.

A1.2.8.   Available capacity and maintenance constraint for thermal generation

Available capacities for thermal generation (*akg*) are calculated by excluding capacities under maintenance from total capacities (Eq. A25). The maintenance schedule is exogenously given as the parameter *UM*, which indicates the rate of plant shutdown under each maintenance schedule. This study assumes four profiles as illustrated in Fig. A1. The model determines the capacity maintained under each schedule (*mkg*).

$$akg_{n,i,d} + \sum_m UM_{m,d} \cdot mkg_{n,i,m} = kg_{n,i} \quad (i = 4, 5, \ldots, 8) \qquad \text{Eq. A25}$$

$$\sum_m UM_{m,d} \cdot mkg_{n,i,m} \geq (1 - MaxAG_i) \cdot kg_{n,i} \quad (i = 4, 5, \ldots, 8) \qquad \text{Eq. A26}$$

$$\sum_m AveUM_m \cdot mkg_{n,i,m} = (1 - AveAG_{n,i}) \cdot kg_{n,i} \quad (i = 4, 5, \ldots, 8) \qquad \text{Eq. A27}$$

$$AveUM_m = \frac{1}{D} \sum_m UM_{m,d} \qquad \text{Eq. A28}$$

where: *UM_{m,d}*: rate of plant shutdown under maintenance schedule *m* (Fig. A1); *AveUM_m*: average rate of plant shutdown under maintenance schedule *m*; *MaxAG_i*: seasonal peak availability of generation type *i*; *AveAG_{n,i}*: annual average availability of generation type *i* at node *n*.
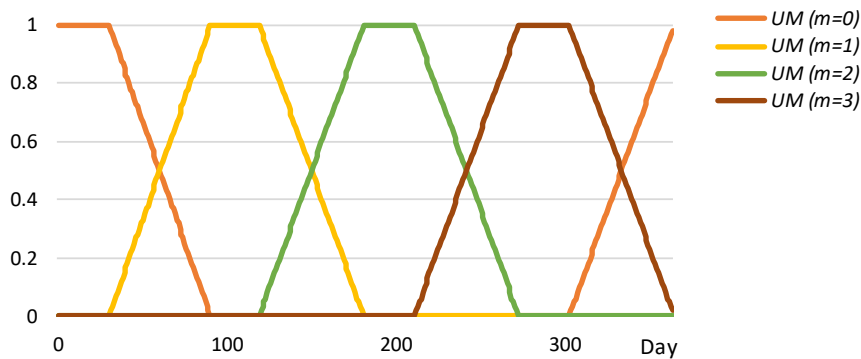

Fig. A1 Rate of plant shutdown under each maintenance schedule

A1.2.9.   CO$_2$ emissions constraint

Eq. A29 constrains the total CO$_2$ emissions in Northeast Asia.

$$\sum_n \sum_i \left(Carbon_i \cdot \sum_d \sum_t \frac{xg_{n,i,d,t} \cdot HW}{EffG_{n,i}} \right) \leq MaxCO2 \qquad \text{Eq. A29}$$

where: *Carbon$_i$*: carbon content of the fuel for generation type *i* [gCO$_2$ per kWh]; *MaxCO2$_i$*: carbon emissions regulation for Northeast Asia [gCO$_2$].

A1.2.10.   Constraint on the maximum SNSP

As mentioned in Section 2.1, this study limits SNSP in each city node from the viewpoint of grid stability. The left part of Eq. A30 indicates the total output from non-synchronous technologies (solar PV, wind, fuel cell, discharge from battery storage and HVDC electricity imports). The right part multiplies the maximum SNSP and the sum of load, charge to pumped hydro and battery, electricity consumption for electrolyzer and electricity exports.

$$\sum_{i \in NSG} xg_{n,i,d,t} + xdc_{n,2,d,t} + \sum_{n2} \sum_l xl_{n2,n,l,DA_{n2,n,d,t},TA_{n2,n,t}}$$

$$\qquad \text{Eq. A30}$$

$$\leq MaxSNSP \cdot \left(L_{n,d,t} + \sum_{s=1}^{2} xch_{n,s,d,t} + \frac{xe_{n,d,t}}{EffE_n} + \sum_{n2} xl_{n,n2,d,t} \right)$$

where: *MaxSNSP*: the maximum SNSP (75%), *NSG*: set of non-synchronous technologies (solar PV, wind and fuel cell).

A1.2.11.   Transmission constraint for supply nodes

Eq. A31 and Eq. A32 requires supply nodes to have enough transmission and/or storage facilities to deliver or store the output of the installed generation capacity in the node. Eq. A31 is for the China-Three Gorges (PRC-TG) node, and Eq. A32 for the China-Uyghur (PRC-UG), the China-Tibet (PRC-TB) and the Mongolia (MN) node. Eq. A33 limits transmission inflow into the supply nodes.

$$\sum_i kg_{n,i} \leq \sum kl_{n,n2,l} \quad (n = 7) \qquad \text{Eq. A31}$$

$$\sum_{i=1}^{2} kg_{n,i} \leq \sum_{n2,l} kl_{n,n2,l} + \sum_{s=1}^{2} ks_{n,s} + ke_n \quad (n = 8, 9, 15) \qquad \text{Eq. A32}$$

$$xl_{n2,n,l,DA_{n2,n,d,t},TA_{n2,n,t}} = 0 \quad (n = 7, 8, 9, 15) \qquad \text{Eq. A33}$$

A1.3.   Detailed assumptions for generation and storage technologies

Fig. A2 depicts initial capacity settings for the generation and storage technologies, and Table A2-Table A8 summarize the economic and technical assumptions. Main sources are as follows: Komiyama, et al. [16] for hydrogen system, METI [17] for pumped hydro and battery, IEA [18] and Komiyama & Fujii [19] for capital

cost for other technologies, and Komiyama & Fujii [19] for technical assumptions of thermal generation (such as ramping capability, share of DSS and minimum output rate). As for capital cost for solar PV in the Mongolia node, this study considers the cost of cleaning sand dust, which was estimated from the cleaning costs in a desert area [31]. Note that "--" in Table A2-Table A8 indicates non-applicable for that technology. Availability factor of hydro and annual average availability of several technologies vary by node and these tables show the range in the country. Assumptions of capital and fuel cost in the Korea node are from those in the Japan nodes in this study.
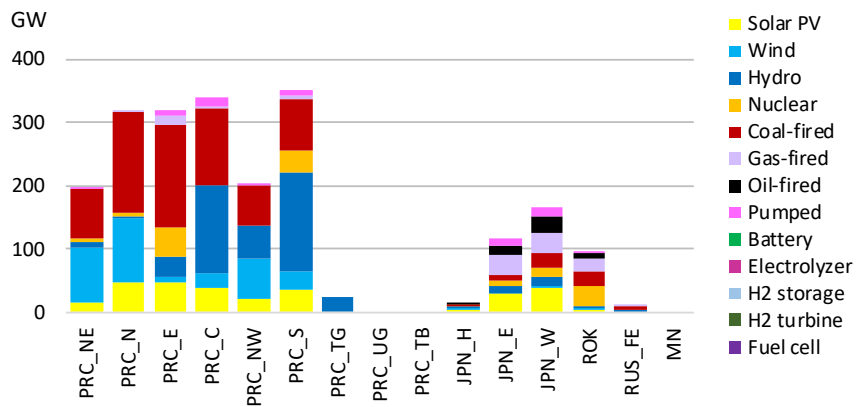
Fig. A2 Initial capacity settings

Table A2 Assumptions for generation technologies (for all nodes)

	Solar PV	Wind	Hydro	Nuclear	Coal-fired	Gas-fired	Oil-fired	H₂ turbine	Fuel cell
Annual fixed charge rate [%]	9.5	11	6.5	8.5	8	8	8	8	9
Carbon content of fuel [MtCO$_2$/Mtoe]	0	0	0	0	3.9	2.4	3.0	0	0
Seasonal peak availability (thermal plants)	--	--	--	95	95	95	95	95	--
Maximum ramp-up rate (thermal plants) [%/h]	--	--	--	0	26	44	44	44	--
Maximum ramp-down rate (thermal plants) [%/h]	--	--	--	0	31	31	31	31	--
Share of DSS operation (thermal plants) [%]	--	--	--	0	0	40	70	40	--
Minimum output level (thermal plants) [%]	--	--	--	80	30	30	30	30	--

Table A3 Assumptions for generation technologies in the China nodes

	Solar PV	Wind	Hydro	Nuclear	Coal-fired	Gas-fired	Oil-fired	H$_2$ turbine	Fuel cell
Capital cost [USD/kW]	1380	1150	3450	2400	750	550	700	550	400
Fuel cost [USD/MWh]	--	--	--	15	12.9	55.9	62.3	--	--
Availability factor (hydro and fuel cell) [%]	--	--	22-72	--	--	--	--	--	80
Annual average availability (thermal plants) [%]	--	--	--	60	60-75	90	75	80	--
Conversion efficiency [%]	--	--	--	100	35	45	39	55	50

Table A4 Assumptions for generation technologies in the Japan nodes

	Solar PV	Wind	Hydro	Nuclear	Coal-fired	Gas-fired	Oil-fired	H$_2$ turbine	Fuel cell
Capital cost [USD/kW]	2400	2000	5200	4000	2500	1100	1900	1100	400
Fuel cost [USD/MWh]	--	--	--	15	17.2	55.9	62.3	--	--
Availability factor (for hydro and fuel cell) [%]	--	--	35	--	--	--	--	--	80
Annual average availability (thermal plants) [%]	--	--	--	65-90	60-85	75-85	75	80	--
Conversion efficiency [%]	--	--	--	100	41	50	39	55	50

Table A5 Assumptions for generation technologies in the Korea node

	Solar PV	Wind	Hydro	Nuclear	Coal-fired	Gas-fired	Oil-fired	H$_2$ turbine	Fuel cell
Capital cost [USD/kW]	2400	2000	5200	4000	2500	1100	1900	1100	400
Fuel cost [USD/MWh]	--	--	--	15	17.2	55.9	62.3	--	--
Availability factor (for hydro and fuel cell) [%]	--	--	40	--	--	--	--	--	80
Annual average availability (thermal plants) [%]	--	--	--	95	90	90	95	80	--
Conversion efficiency [%]	--	--	--	100	37	51	39	55	50

Table A6 Assumptions for generation technologies in the Russia Far East node

	Solar PV	Wind	Hydro	Nuclear	Coal-fired	Gas-fired	Oil-fired	H$_2$ turbine	Fuel cell
Capital cost [USD/kW]	1400	1930	4550	3800	2100	800	1900	800	400
Fuel cost [USD/MWh]	--	--	--	15	12.9	38.7	62.3	--	--
Availability factor (hydro and fuel cell) [%]	--	--	33	--	--	--	--	--	80
Annual average availability (thermal plants) [%]	--	--	--	80	75	75	75	80	--
Conversion efficiency [%]	--	--	--	100	35	35	39	55	50

Table A7 Assumptions for generation technologies in the Mongolia node

	Solar PV	Wind	H_2 turbine	Fuel cell
Capital cost [USD/kW]	1430	1150	800	400
Availability factor (fuel cell) [%]	--	--	--	80
Annual average availability (hydrogen turbine) [%]	--	--	80	--
Conversion efficiency [%]	--	--	55	50

Table A8 Assumptions for storage technologies and electrolyzer (for all nodes)

	Pumped hydro	Battery	Compressed H_2 tank	Electrolyzer
Capital cost for kW-capacity [USD/kW]	--	--	700	400
Capital cost for kWh-capacity (storage) [USD/kWh]	230	400	15	--
Annual fixed charge rate [%]	6.5	9	9	9
Availability factor [%]	80	80	80	80
Cycle efficiency (storage) [%]	70	85	90	--
Self-discharge loss (storage) [%/h]	0.01	0.1	0.01	--
Non-durable material cost (storage)	0	35	0	--
kWh-capacity ratio to kW-capacity (pumped and battery)	6	6	--	--
Conversion efficiency (electrolyzer) [%]	--	--	--	70

Appendix 2.   Assumed electricity load curves for China

Historic load curves for a year in China are not publicly available. Therefore, this paper estimated hourly load curve for each Chinese city node in the following three steps. First, daily electricity consumption D_d [GWh] was estimated at each node, using actual temperature data in major cities [21] and relationships between temperature and daily electricity consumption [32, 33]. Second, a reference load pattern was estimated for each day $RL_{d,t}$ by using a weighted average of available seasonal load curves [34, 35, 36]. Note that $RL_{d,t}$ indicates the share of electricity consumption in each time slot of the day. Then, this paper developed a linear programming model, as summarized in Eq. A34-Eq. A39 to estimate the hourly load curve for a year by adjusting a reference load curve ($D_d \times RL_{d,t}$). The model aims to minimize adjustment penalties under various constraints, including a daily consumption constraint (Eq. A36), annual load factor constraint (Eq. A37-Eq. A38) and continuity constraint (Eq. A39).

Table A9 Endogenous variables of the load estimation model

z	Sum of adjustment penalties
$Load_{d,t}$	Adjusted load curve [GW]
$peak$	Annual peak load of the adjusted load curve [GW]
$du_{d,t,sp}$, $dl_{d,i,sp}$	Variables to adjust the reference load curve ($D_d \times RL_{d,t}$) upward and downward, respectively ($0 \leqq du_{d,t,sp} \leqq 0.025$, $0 \leqq dl_{d,t,sp} \leqq 0.025$)

where:

d: *day index* $(0, 1, \ldots, 364 \text{ or } 365)$, t: *time index* $(0, 1, \ldots, 23)$,

sp: *adjustment step index* $(0, 1, \ldots, 19 \text{ in this study})$

A2.1. Objective function

This model aims to minimize the sum of adjustment penalties.

$$min. \ z = \sum_{d} \sum_{t} \sum_{sp} Pe_{sp} \cdot (du_{d,t,sp} + dl_{d,t,sp})$$

Eq. A34

where: Pe_{sp}: adjustment penalties [/GW]. This study assumes that $Pe_{sp}=(SP+1)^2$ ($Pe_0=1$, $Pe_1=4$, … , $Pe_{19}=400$).

A2.2. Constraints

A2.2.1. Load adjustment equation

This equation is to adjust the reference load curve. $du_{d,t,sp}$ and $dl_{d,t,sp}$ in the right side are the variables for adjustment.

$$load_{d,t} = D_d \cdot RL_{d,t} \cdot \left\{ 1 + \sum_{sp} (du_{d,t,sp} - dl_{d,t,sp}) \right\}$$

Eq. A35

where: D_d: Daily electricity consumption [GWh]; $RL_{d,t}$: reference load pattern (in a ratio to the daily electricity consumption).

A2.2.2. Daily consumption constraint

This constraint ensures that the daily summation of adjusted load ($Load_{d,t}$) is equal to the estimated daily consumption (D_d).

$$D_d = \sum_{t} load_{d,t}$$

Eq. A36

A2.2.3. Annual load factor constraint

This constraint limits the annual load factor, the ratio between average load and peak load, within the specified range.

$$load_{d,t} \leq peak \qquad \text{Eq. A37}$$

$$MinLF \leq \sum_d \sum_t \frac{load_{d,t}}{ND \cdot NT \cdot peak} \leq MaxLF \qquad \text{Eq. A38}$$

where: *MinLF*: Lower bound for adjusted load factor; *MaxLF*: Upper bound for adjusted load factor; *ND*: The number of day (*ND* = 365 or 366); *NT*: The number of time slices in the day (*NT* = 24).

A2.2.4. Continuity constraint

This constraint is for smoothing the adjusted load across the day.

$$load_{d,23} \cdot (1 - CL) \leq load_{d+1,0} \leq load_{d,23} \cdot (1 + CL) \qquad \text{Eq. A39}$$

where: *CL*: Continuity coefficient

This paper validated the estimated load curves using the best available data (Fig. A3-Fig. A5). Fig. A3 compares quarterly power generation in China [37] with estimated consumption calculated by $load_{d,t}$. Generation and estimated consumption are expressed in a ratio to the annual total. Note that, in a strict sense, generation and consumption are not comparable; yet, due to data availability, generation data was used as a proxy in this validation. Fig. A3 implies that seasonality, such as increasing generation in summer (July-September), is well captured in the estimated consumption.

Load duration curves in several areas or provinces are available in China; therefore, this study also validated the estimated load curves on a duration-curve basis. Fig. A4 compares the estimated curve for China-North with the actual load duration curves in the Beijing-Tianjin-Tangshan area. Fig. A5 illustrates China-South and actual data in Yunnan province. These figures also imply that the estimated curves well reproduce the actual consumption trends.
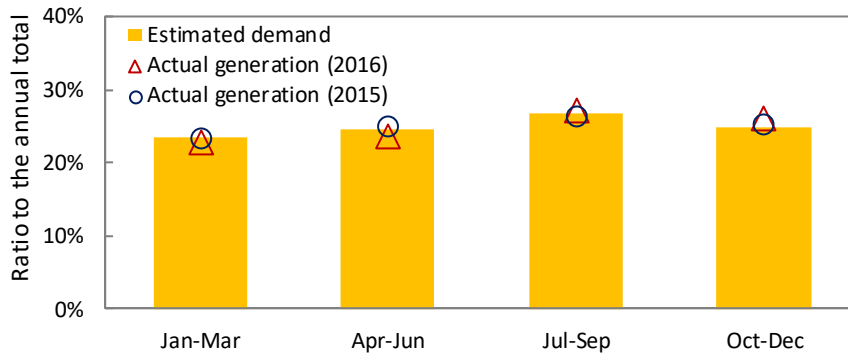

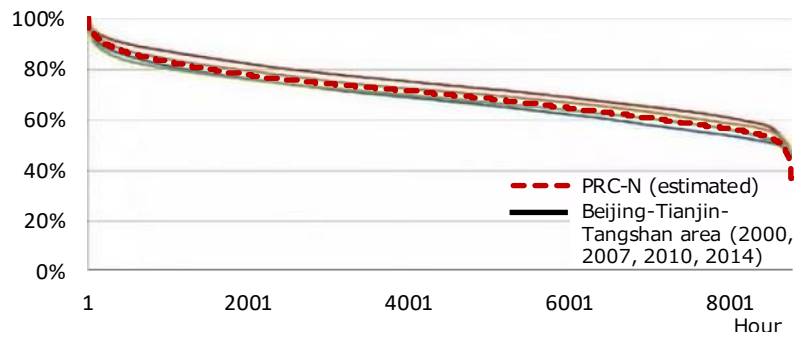Fig. A3 Comparison between quarterly generation and estimated consumption in China

Fig. A4 Comparison between historic load duration curves in Beijing-Tianjin-Tangshan area
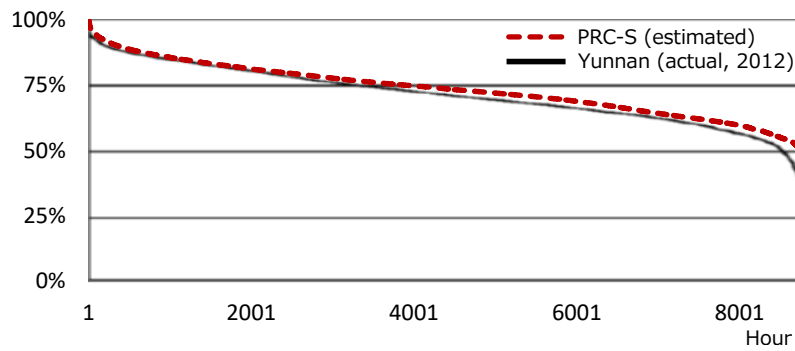
and estimated curve for the China-North node

Fig. A5 Comparison between a historic load duration curve in Yunnan province

and estimated curve for the China-South node

References

[1]   E. Charter, KEEI, E. RAS, M. o. Mongolia and JREF, "Gobitec and Asian Super Grid for Renewable Energies in Northeast Asia," Energy Charter Secretariat, ISBN 978-905948-143-5, 2014.

[2]   KEPCO, "KEPCO's Future Plans of Northeast Asia Supergrid," 2014. [Online]. Available: http://www.energycharter.org/fileadmin/DocumentsMedia/Forums/ECF_Ulaanbaatar_2014_ S2_Kwang_Hee.pdf. [Accessed 17 Oct 2016].

[3]   SGCC, "Connotation and Outlook of Global Energy Interconnection," 2016. [Online]. Available: https://www.renewable-ei.org/images/pdf/20160525/Special_address2_Wan_Haibin.pdf. [Accessed 17 Oct 2016].

[4]   L. Belyaev, N. Voropai, S. Podkovalnikov and G. Shutov, "Problems of power grid formation in Northeast Asia," *Elektrichestvo,* vol. 2, pp. 15-27, 1998.

[5]   K. H. Chung and B. H. Kim, "Economic Feasibility on the Interconnected Electric Power Systems in North-East Asia," *Journal of Electrical Engineering & Technology,* vol. 2, no. 4, pp. 452-460, 2007.

[6]   T. Otsuki, A. B. Mohd Isa and R. Samuelson, "Electric power grid interconnections in Northeast Asia: A quantitative analysis of opportunities and challenges," *Energy Policy,* vol. 89, pp. 311-329, 2016.

[7]   D. Bogdanov and C. Breyer, "North-East Asian Super Grid for Grid for 100% renewable energy supply: Optimal mix of energy technologies for electricity, gas and heat supply options," *Energy Conversion and Management,* vol. 112, pp. 176-190, 2016.

[8]   T. Otsuki, "Costs and benefits of large-scale deployment of wind turbines and solar PV in Mongolia for international poewr exports," *Renewable Energy,* vol. 108, pp. 321-335, 2017.

[9]   R. Komiyama, T. Otsuki and Y. Fujii, "Energy modeling and analysis for optimal grid integration of large-scale variable renewables using hydrogen storage in Japan," *Energy,* vol. 81, pp. 537-555, 2015.

[10]   EirGrid, "Ensuring a Secure Reliable and Efficient Power System in a Changing Environment," EirGrid, 2011.

[11]   EirGrid, "DS3 Programme Operational Capability Outlook 2016," EirGrid, 2016.

[12]   GOJ, "Setsuden.go.jp," 2015. [Online]. Available: http://setsuden.go.jp/. [Accessed 13 Mar 2015].

[13]   S. UPS, "Generation and consumption," 2016. [Online]. Available: http://www.so-cdu.ru/. [Accessed 17 Oct 2016].

[14] KPX, "Power system operation information," 2016. [Online]. Available: http://www.kpx.or.kr/www/contents.do?key=20. [Accessed 17 Oct 2016].

[15] APERC, "APEC Energy Demand and Supply Outlook 6th Edition," APEC#216-RE-01.8, ISBN 978-981-09-8921-7, 2016.

[16] R. Komiyama, T. Otsuki and Y. Fujii, "Optimal Power Generation Mix considering Hydrogen Storage of Variable Renewable Power Generation," *IEEJ Transactions on Power and Energy,* vol. 134, no. 10, pp. 885-895 (in Japanese), 2014.

[17] METI, "Battery strategies," 2012. [Online]. Available: http://www.enecho.meti.go.jp/committee/council/basic_problem_committee/028/pdf/28sankou2-2.pdf. [Accessed 17 Oct 2016].

[18] IEA, "WEO - Investment Costs," 2016. [Online]. Available: http://www.worldenergyoutlook.org/weomodel/investmentcosts/. [Accessed 17 Oct 2016].

[19] R. Komiyama and Y. Fujii, "Assessment of post-Fukushima renewable energy policy in Japan's nation-wide power grid," *Energy Policy,* vol. 101, pp. 594-611, 2017.

[20] NREL, "Meteorology: typical meteorological year data for selected stations in China from NREL," 2016. [Online]. Available: https://catalog.data.gov/dataset/meteorology-typical-meteorological-year-data-for-selected-stations-in-china-from-nrel-af0da. [Accessed 17 Oct 2016].

[21] JMA, "Automated Meteorological Data Acquisition System," Japan Meteorological Agency (in Japanese), 2015.

[22] KMA, "Current Weather," 2016. [Online]. Available: http://www.kma.go.kr/weather/observation/currentweather.jsp. [Accessed 10 Jul 2016].

[23] NREL, "PV Watts Calculator," 2017. [Online]. Available: http://pvwatts.nrel.gov/. [Accessed 7 Mar 2017].

[24] G. He and D. M. Kammen, "Where, when and how much wind is available? A provincial-scale wind resource assessment for China," *Energy Policy,* vol. 74, pp. 116-122, 2014.

[25] G. He and D. M. Kammen, "Where, when and how much solar is available? A provincial-scale solar resource assessment for China," *Renewable Energy,* vol. 85, pp. 74-82, 2016.

[26] MOE, "Study on Basic Zoning Information Concerning Renewable Energies (FY2015)," (in Japanese, "平成 27 年度再生可能エネルギーに関するゾーニング基礎情報整備告書"), 2016.

[27] KOPIA, "Study on potential solar power deployment capacity," (in Korean), 2011.

[28] H.-G. Kim, Y.-H. Kang, H.-J. Hwang and C.-J. Yun, "Evaluation of Inland Wind Resource Potential of South Korea According to Environmental Conservation Value Assessment,"

Energy Procedia, vol. 577, pp. 773-781, 2014.

[29] D. Elliott, M. Schwartz, G. Scott, S. Haymes, D. Heimiller and R. George, "Wind Energy Resource Atlas of Mongolia," NREL/TP-500-28972, 2001.

[30] Q. Chen, C. Kang, H. Ming, Z. Wang, Q. Xia and G. Xu, "Assessing the low-carbon effects of inter-regional energy delivery in China's electricity sector," *Renewable and Sustainable Energy Reviews,* vol. 32, pp. 671-683, 2014.

[31] SASIA, "Desert Protocol Tests to be Required for PV in Saudi Arabia," 2016. [Online]. Available: http://saudi-sia.com/desert-protocol-tests-to-be-required-for-pv-in-saudi-arabia/. [Accessed 25 Jun 2016].

[32] Z. Y. Zhang, D. Y. Gong and J. J. Ma, "A study on the electric power load of Beijing and its relationships with meteorological factors during summer annd winter," *Meteorological Applications,* vol. 21, pp. 141-148, 2014.

[33] Y.-L. Hou, H.-Z. Mu, G.-T. Dong and J. Shi, "Influences of Urban Temperature on the Electricity Consumption of Shanghai," *Advances in Climate Change Research,* vol. 5, no. 2, pp. 74-80, 2014.

[34] JEPIC, "Overseas electric power industry statistics 2006," 2006.

[35] C. Cheng, "Electricity Demand-Side Management for an Energy Efficient Future in China: Technology Options and Policy Priorities," Ph.D Dissertation. Massachusetts Institute of Technology, 2005.

[36] P. Duan, K. Xie, T. Guo and X. Huang, "Short-Term Load Forecasting for Electric Power Systems Using the PSO-SVR and FCM Clustering Techniques," *Energies,* vol. 4, pp. 173-184, 2011.

[37] NBS, "National Data - Monthly - Energy - Output of Electricity," 2017. [Online]. Available: http://data.stats.gov.cn/english/index.htm. [Accessed 12 Jun 2017].

[38] IRENA, "Planning for the renewable future," ISBN 978-92-95111-06-6, 2017.